American Mineralogist, Volume 81, pages 67–78, 1996

Ordering of the stacking sequence in cookeite with increasing pressure: An HRTEM study*

MICHEL JULLIEN,[1] ALAIN BARONNET,[2] AND BRUNO GOFFÉ[1]

[1]Laboratoire de géologie, URA 1316 du CNRS, Ecole Normale Supérieure, 24 rue Lhomond, 75231 Paris cedex 05, France
[2]Centre de recherche sur les mécanismes de la croissance cristalline, CRMC²-CNRS, Campus de Luminy, Case 913, 13288 Marseille cedex 09, France

ABSTRACT

To explore the effect of pressure on the stacking-sequence of the chlorite cookeite, a systematic TEM study of stacking microstructures has been conducted on natural samples from pegmatitic and metamorphic environments representing a large pressure field over a relatively narrow temperature range. The low-*P* and low-*T* conditions (1–5 kbar, 280–350 °C) are represented by late-crystallized cookeite from pegmatites and by cookeite from low-temperature metapelites. For the high-*P* conditions (5–16 kbar, 280–430 °C), cookeite samples from metapelites and metabauxites were selected. Combining selected-area electron diffraction (SAED) and high-resolution transmission electron microscopy (HRTEM) imaging shows that the polytypes evolve from a fully semirandom type to fully ordered types under increasing total pressure. For both polytypes the repeat distance (from one to five layers) of the basic structures and the diversity of repeats increase with pressure. Above 10 kbar, long-period polytypes (LPP), up to at least a 14-layer repeat, coexist with perfectly ordered basic structures. Neither the unique type of intralayer stacking (*Ia*) nor the single-layer subcell volume measurements improve understanding of the role of pressure on the ordering process. Clearly, the regular polytypes of cookeite behave as polymorphs that are remarkably sensitive to total pressure.

INTRODUCTION

Cookeite is a di-trioctahedral chlorite of ideal formula $LiAl_4Si_3AlO_{10}(OH)_8$ (Brammal et al. 1937). It is usually found as a late, low-pressure, low-temperature alteration product of various Li-bearing minerals such as spodumene, petalite, and lepidolite in pegmatitic and hydrothermal environments (Lacroix 1915; Cerny 1970; Cerny et al. 1971). Cookeite also occurs frequently in a wide variety of metamorphic rocks, dominantly at low temperatures. It has been reported in low-temperature, low-pressure metapelites (Theye 1992 personal communication; Jullien and Goffé 1993; Bouybaouène 1993; Azañon 1994; Goffé et al. 1996), in medium-temperature, medium-pressure metabauxites (Sartori 1988), in medium-temperature, low-pressure metabauxites (Vrublevskaja et al. 1975), and in low- to medium-temperature, high-pressure metapelites and metabauxites (Goffé 1977, 1979, 1980, 1982, 1984; Goffé et al. 1987, 1994, 1996; Theye 1988; Bouybaouène 1993; Azañon 1994).

Polytypism of chlorite's unit cell is well known from numerous X-ray studies (Brown and Bailey 1962, 1963; Shirozu and Bailey 1965; Eggleton and Bailey 1967; Lister and Bailey 1967; Bailey 1980, 1988; Vrublevskaja et al. 1975; Spinnler et al. 1984; Bailey and Lister 1989). Investigation of detailed stacking sequences in chlorites requires high-resolution transmission electron microscopy (HRTEM) observations, which to date have been obtained in only a few studies (Schreyer et al. 1982; Veblen and Ferry 1983; Veblen 1983; Maresch et al. 1985; Bons and Schryvers 1989; Ferrow et al. 1990). These works are restricted to essentially disordered trioctahedral species, although Schreyer et al. (1982) reported a five-layer sequence in clinochlore. The report of perfectly ordered two-layer cookeite in very-low-temperature, high-pressure metapelites (Goffé et al. 1994) suggests that such regular polytypes could be related to high-pressure, low-temperature conditions. More generally, this observation raises the question of the intrinsic influence of pressure on polytypism.

Factors that are likely to influence the layer stacking sequence and polytypism in sheet silicates include temperature, pressure, crystal-growth mechanisms, and the chemical composition of the single layer. Temperature, crystal-growth mechanisms, and composition are know to influence polytypism. The effect of confining pressure has never been demonstrated, whereas deformation has recently been shown to order polytypic structures in the case of serpentines (Banfield et al. 1995).

Among polytypic layer silicates, cookeite appears as a possible candidate for investigation of the intrinsic effect of pressure on polytypism. With the exception of the crystal-growth mechanisms, which are largely unknown, the

* Dedicated to the memory of Professor Sturges W. Bailey.

0003–004X/96/0102–0067$05.00

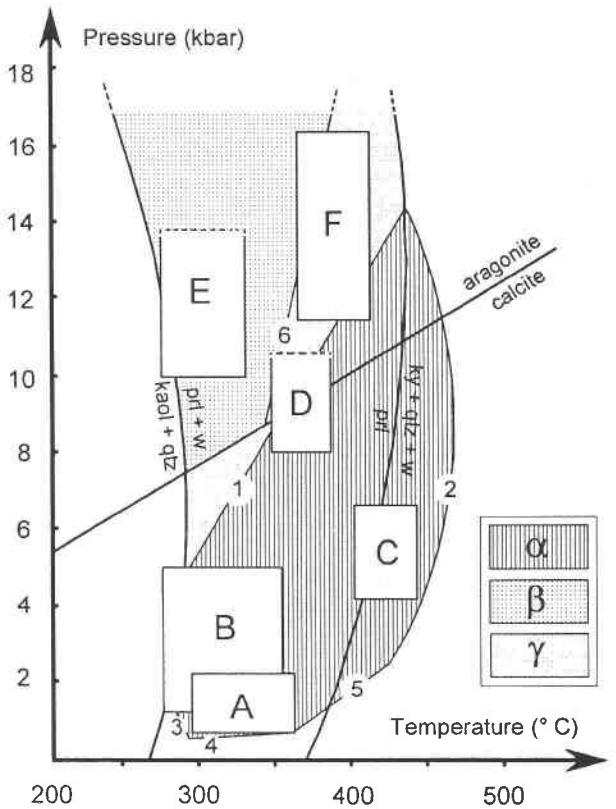

FIGURE 1. *P-T* diagram showing the conditions of formation of cookeite samples examined in this study. Symbols are as follows: α = calculated stability field of the association cookeite + quartz, after Vidal and Goffé (1991); β = metamorphic *P-T* conditions for rocks that contain the association cookeite + saliotite, estimated using Reaction 6, after Goffé et al. (1994); γ = cookeite + quartz stability in the field of spodumene (see text). Reactions in the LASH system (Vidal and Goffé 1991) limiting the stability field cookeite + quartz: 1 = cookeite + quartz → spodumene + pyrophyllite + H_2O; 2 = cookeite + quartz → spodumene + kyanite + H_2O; 3 = cookeite + quartz → bikitaite + pyrophyllite + H_2O; 4 = cookeite + quartz → petalite + pyrophyllite + H_2O; 5 = cookeite + quartz → petalite + andalusite + H_2O. Reaction in the FMASH system (Vidal et al. 1992): 6 = carpholite → chloritoid + quartz + H_2O.

other parameters may be considered as approximately fixed. The dioctahedral chlorite cookeite is remarkably constant in composition in comparison with trioctahedral chlorites. Its stability field, established by Vidal and Goffé (1991), exhibits a large pressure extent, from 1 to 16 kbar, over a narrow temperature range, between 280 and 450 °C.

This work attempts to characterize the stacking sequence in cookeite as a function of pressure. We studied this layer stacking sequence using HRTEM imaging, selected-area electron diffraction (SAED), and analytical electron microscopy (AEM) techniques. In addition, we used X-ray diffraction to determine unit-cell volumes and each cookeite structural type as defined by Brown and Bailey (1962). The conditions of formation were determined by independent petrological techniques using metamorphic paragenesis and thermodynamic calculations. They correspond to a large range of pressure conditions over a narrow range of temperature.

EXPERIMENTAL TECHNIQUES

Chemical analyses were performed with the Camebax and SX50 electron microprobes (Cameca) at the University of Paris VI (15 kV, 10 nA beam conditions) using Fe_2O_3 (Fe), $MnTiO_3$ (Ti), diopside (Mg,Si), orthoclase (K,Al), albite (Na), and anorthite (Ca) as standards, with an electron-beam diameter of approximately 2 μm. Li analyses were made using the ion microprobe (Cameca) at Nancy CRPG using lepidolite, zinnwaldite, and cookeite previously analyzed by B. Goffé, as Li standards.

HRTEM was performed using a JEOL 2000FX transmission electron microscope (200 kV accelerating voltage, side-entry, double-tilt (±30°) HR specimen holder, point-to-point resolution of 2.8 Å). TEM specimens were extracted from standard petrographic thin sections (30 μm thick) glued by Lakeside resin onto a glass slide. Microdrilling of 3 mm disks was performed on selected areas, and single-hole copper TEM grids were glued onto them with a thin film of Araldite resin. The specimen was carefully removed from the thin section with tweezers after gently heating the Lakeside resin and then thinned to perforation by ion-beam milling (IMMI-5, GATAN 600 Duomill, 5 kV, argon beam).

We explored and characterized each sample by SAED before recording one- or two-dimensional lattice images using HRTEM. Diffraction and imaging techniques were similar to those detailed in Baronnet (1992).

The same electron microscope was operated at 200 kV for HRTEM imaging, electron diffraction, and microanalyses. AEM was performed with a Tracor Northern energy-dispersive (EDS) X-ray spectrometer [TN5502, series II, Si(Li) detector with a Be window] with raw data reduced by the SMTF (standardless microanalysis of thin films) procedure similar to the original Cliff and Lorimer method (Cliff and Lorimer 1975). Experimental $k_{x,Si}$ factors were calibrated against layer-silicate standards (Cliff and Lorimer 1975; Mellini and Menichini 1985). In fixed transmission mode, the analytical spot-size diameter ranged from 200 to 800 Å to limit beam damage on the minerals. These analyses are qualitative to semiquantitative and allowed us to identify the mineral species under the electron microscope, mainly by their Al/Si atomic ratio.

The high Li and OH contents of cookeite make it very unstable under the electron beam. To avoid these difficulties we used a low-light camera (LHESA EM LH 4086) equipped with a YAG converter to explore the TEM grid and optimize the imaging conditions under very low illumination. HRTEM images were recorded after rapid focusing of the electron beam.

X-ray diffraction powder patterns were obtained using a 114.6 mm Gandolfi camera with Cu$K\alpha$ radiation and indexed after Bailey and Lister (1989). Unit-cell param-

TABLE 1. Sample characterization and petrologic data relevant to the *P-T* conditions of cookeite formation

Group	Rock types and area	Geological setting of cookeite samples	Minerals associated with cookeite	Index minerals in neighboring rocks, metamorphic paragenesis	*P-T* conditions and geotherm	Ref.
F	Metapelites and metabauxites. Western Crete, phyllite-quartzite unit (Greece).	Cookeite occurs in rocks and in associated synfolial quartz segregations.	Diaspore or quartz, pyrophyllite, chloritoid, lawsonite, phengite, paragonite, calcite, hematite.	Glaucophane, Fe- and Mg-rich carpholite, chloritoid, paragonite, aragonite. Blueschist facies. Relic of saliotite.	P = 12–17 kbar T = 370–400°C 8–9°/km	9
E	Metapelites. Betic chain, Eastern Alpujarrides, Alhamilla unit (Spain).	Early synfolial cookeite occurs in quartz segregations, in equilibrium with pyrophyllite, aragonite, and saliotite. Replacement of partially retrotemperatured saliotite by paragonite, cookeite, and calcite.	Quartz, pyrophyllite, saliotite, paragonite, phengite, aragonite, calcite, ankerite.	Mg-rich carpholite, aragonite, kaolinite; very-low-temperature blueschist facies.	P > 10–12 kbar T = 280–330 °C 9–10°/km	8
D	Metabauxites. Western Alps, Briançonnais cover, Ligurian Alps (Italy).	Associated with the other sheet silicates in the main foliation of the rocks. It can be included in Mg-rich carpholite. It does not occur in the associated veins.	Diaspore or quartz, pyrophyllite, Fe-rich chloritoid, Fe- and Mg-rich carpholite, chlorite, phengite, paragonite, hematite.	Glaucophane, lawsonite. Blueschist facies followed by a cooling decompression *P-T*–path.	P > 8–10 kbar T = 350–380 °C 11°/km	7
	Metabauxites. Western Alps, Briançonnais cover, Western Vanoise (France).	Cookeite occurs in rocks and veins.	Diaspore or quartz, pyrophyllite, Fe-rich chloritoid, Fe- and Mg-rich carpholite, chlorite, lawsonite, phengite, paragonite, ankerite, hematite.	Lawsonite, aragonite. Blueschist facies followed by a cooling decompression *P-T*–path.	P = 8–10 kbar T = 350–380 °C 13°/km	6
C	Metabauxites. Western Alps, Briançonnais cover, Barrhorn (Switzerland).	In equilibrium in the paragenesis or associated with pyrophyllite as a late breakdown product of kyanite.	Diaspore, pyrophyllite, kyanite, Fe-rich chloritoid, chlorite, Zn-rich staurolite, epidote, margarite, paragonite, muscovite, calcite.	Green amphibole, garnet, albite, chlorite; medium- to high-temperature greenschist facies.	P = 4–6 kbar T = 400–450 °C 28°/km	5
B	Metapelites. Western Alps, Dauphinois zone (France).	Intimately intergrown with the other sheet silicates in synfolial quartz segregations.	Quartz, pyrophyllite, chlorite, phengite, paragonite, margarite, calcite.	Low-temperature greenschist facies.	P = 1–5 kbar T = 270–340 °C 33°/km	4
	Metapelites. Rif chain, Sebtides, Tizgarine unit (Morocco).	Intimately intergrown with muscovite and chlorite in synfolial quartz segregations.	Quartz, chlorite, muscovite, paragonite, calcite.	Low-temperature greenschist facies.	P = 1–3 kbar T = 300 °C 50°/km	3
	Metapelites. Variscan belt; Western Brittany, Plougastel (France).	Hercynian syntectonic veins.	Quartz, chlorite, muscovite, calcite.	Pyrophyllite, chlorite; low-temperature greenschist facies.	P = 1–2 kbar T = 300 °C 60°/km	2
A	Pegmatites. Dobra Voda (Czech Republic); Castelnau de Brassac (Tarn, France); Greenwood (Maine, U.S.A.).	Related to granitic intrusion. Late growing, precipitated from late hydrothermal fluid alteration of Li-bearing minerals such as rubellite or spodumene.	Quartz, lepidolite, muscovite, albite, rubellite, F-rich apatite, cassiterite, topaz, garnet.	Low-pressure, low-temperature conditions.	P = 1–1.5 kbar T = 300–350 °C 90°/km	1

Note: References are as follows: 1 = Cerny et al. 1971; Arsandaux 1901; Penfield 1894; 2 = Paradis et al. 1983; Theye 1992 personal communication; 3 = Goffé et al. 1996; 4 = Jullien and Goffé 1993; 5 = Sartori 1988; 6 = Goffé 1977, 1979, 1982; Goffé et al. 1987; Saliot and Velde 1982; Gillet and Goffé 1988; 7 = Goffé 1980, 1982, 1984; Messiga et al. 1982; 8 = Goffé et al. unpublished data; Goffé et al. 1994, 1996; and 9 = Theye 1988; Theye et al. 1992; Jolivet et al. 1996.

eters and volumes were refined using the Appleman and Evans (1973) program.

SAMPLE LOCALITIES, DESCRIPTIONS, AND MINERAL CHEMISTRY

Sample localities

To assess the influence of pressure on cookeite microstructures, we chose 11 samples from six *P-T* domains corresponding to six typical *P-T* conditions (groups A–F, Fig. 1, Table 1) ranging between 1 and 16 kbar and approximately 300–400 °C. The *P-T* determinations for each group of samples (Fig. 1), and thus the representative geotherms, are based on previous work (see references in Table 1) and our ongoing studies. In Figure 1, the *P-T* location of each group of samples is an average of these data, reported in Table 1.

For low-temperature, low-pressure conditions, three cookeite samples from pegmatitic environments [group A; Dobra Voda (Western Moravy, Czeck Republic), Greenwood (Maine, U.S.A.), and Castelnau de Brassac (Tarn, France)] and three metamorphic samples [group

Table 2. Representative chemical analyses of cookeite samples from groups A–F

Analyses	A			B			C	D	E	F	
Sample	Dobra	Cast.	Green.	Britt.	Tiz.	Dauph.	Barrh.	Van.	Alh.	Crete1	Crete2
SiO_2	32.71	37.98	36.68	34.98	34.60	35.42	35.12	36.70	33.66	36.88	35.16
TiO_2	0.00	0.01	0.01	0.00	0.01	0.00	0.16	0.00	0.00	0.00	0.03
Al_2O_3	43.19	45.63	46.72	45.85	43.61	44.31	44.48	47.35	43.88	47.92	45.30
FeO	0.00	0.00	0.05	1.30	1.12	0.20	0.63	0.81	0.43	0.62	0.01
MnO	0.00	0.00	0.04	0.00	0.03	0.00	0.04	0.00	0.04	0.03	0.02
MgO	0.00	0.03	0.01	0.07	1.16	0.14	0.92	0.31	0.09	0.07	0.04
CaO	0.02	0.01	0.03	0.02	0.08	0.06	0.09	0.00	0.04	0.05	0.07
Na_2O	0.02	0.01	0.00	0.00	0.09	0.02	0.05	0.00	0.15	0.04	0.18
K_2O	0.07	0.01	0.02	0.02	0.07	0.02	0.15	0.00	0.07	0.04	0.06
Li_2O	3.87	n.a.	n.a.	n.a.	1.95	2.75	1.68	2.14	2.28	n.a.	n.a.
Total	79.88	81.07	81.07	82.40	82.72	82.92	83.33	87.31	80.64	85.73	81.07
O	14.00	13.50	13.50	13.50	14.00	14.00	14.00	14.00	14.00	13.50	13.50
					Atoms per formula unit						
Si	3.060	3.272	3.172	3.102	3.163	3.196	3.179	3.161	3.137	3.127	3.147
Ti	0.000	0.001	0.001	0.000	0.001	0.000	0.011	0.000	0.000	0.000	0.002
Al	4.762	4.633	4.762	4.792	4.699	4.711	4.745	4.806	4.819	4.788	4.779
Fe^{2+}	0.000	0.000	0.004	0.096	0.086	0.015	0.048	0.058	0.034	0.044	0.001
Mn	0.000	0.000	0.003	0.000	0.002	0.000	0.003	0.000	0.003	0.002	0.002
Mg	0.000	0.004	0.001	0.009	0.158	0.019	0.123	0.040	0.013	0.009	0.005
Ca	0.002	0.001	0.003	0.002	0.008	0.006	0.009	0.000	0.004	0.005	0.007
Na	0.004	0.002	0.000	0.000	0.016	0.003	0.009	0.000	0.027	0.007	0.031
K	0.009	0.001	0.002	0.002	0.008	0.002	0.018	0.000	0.008	0.004	0.007
Li	1.456	n.a.	n.a.	n.a.	0.717	0.998	0.612	0.741	0.854	n.a.	n.a.
Total	23.29	21.41	21.45	21.50	22.86	22.95	22.76	22.81	22.90	21.48	21.50

Note: For analytical techniques and standards, see text; n.a. = not analyzed. Dobra = Dobra Voda, pegmatite, Czeck Republic; Cast. = Castelnau de Brassac, pegmatite, France; Green = Greenwood, pegmatite, U.S.A.; Britt. = Brittany, metapelite, France; Tiz. = Tizgarine, metapelite, Morocco; Dauph. = Dauphinois, metapelite, France; Barrh. = Barrhorn, metabauxite, Switzerland; Van. = Vanoise, metabauxite, France; Alh. = Alhamilla, metapelite, Spain; Crete1 = metabauxite, Greece; Crete2 = metapelite, Greece.

B; Tizgarine (Rif Chain, Morocco), Dauphinois zone (Isère, France), and Brittany (France)] were selected. For the higher pressure conditions, we used five metamorphic samples from four *P-T* domains [groups C–F); from low to high pressure: Barrhorn (Switzerland), Vanoise (France), Alhamilla (Betic Chain, Spain), and Western Crete (Greece).

Geological setting

The pegmatite from Dobra Voda (group A) was described by Cerny et al. (1971). Cookeite occurs in pearly white, fine-grained, lamellar clusters and in micrometer- to millimeter-sized radial rosettes around lepidolite. In the Maine sample, as in the Tarn, the cookeite is located at the alteration boundary of either rubellite or spodumene (Lacroix 1915) and is associated with lepidolite, quartz, and apatite. The crystallization of these cookeite samples occurred during the last stage of the hydrothermal alteration of pegmatites.

We studied three metamorphic samples from low-temperature greenschist facies (group B) formed between 1 and 5 kbar and 300–350 °C. Cookeite from Tizgarine metapelites (Morocco) occurs in fine intergrowths associated with muscovite and chlorite. In the Dauphinois zone (Jullien and Goffé 1993), cookeite appearance is restricted to the Aalenian metapelites (black shales), in fine intergrowths with other phyllosilicates. The sample from Brittany is the sole cookeite in this study that did not undergo Alpine metamorphism. These Devonian schists were metamorphosed during the Hercynian multiphase orogenesis.

Metamorphic group C corresponds to the high-temperature greenschist facies (Table 1) represented by a sample of metabauxite from Barrhorn (Briançonnais cover, Western Alps, Switzerland). The *P-T* formation conditions determined by Sartori (1988) are highly constrained by the paragenesis (Table 1).

Two samples from the blueschist facies, Western Vanoise and Liguria (group D), are from the same geological unit (the Briançonnais cover) that the Barrhorn sample is from, with the same metabauxite bulk composition. The presence of ferromagnesian carpholite and aragonite is evidence for higher pressures. In the Vanoise sample, the *P-T* conditions (8–10 kbar, 350–380 °C) are well constrained by the association of cookeite with index minerals such as Fe-rich chloritoid, Fe- and Mg-rich chlorite, and lawsonite (Table 1) in the paragenesis. The preservation of high-pressure phases during exhumation is explained by cooling during decompression, a common *P-T* path for the Briançonnais cover (see Table 1 for references). In the Ligurian sample, the appearance of glaucophane reveals pressures higher than those in the Vanoise sample ($P > 8$–10 kbar) and accounts for the lack of an upper pressure limit for the *P-T* group D shown in Figure 1.

The sample from Alhamilla (group E, Fig. 1) displays a dramatic contrast between pressure and temperature ($P > 10$–12 kbar, $T = 280$–320 °C) in the very-low-temperature blueschist facies. In this case, the influence of

pressure is magnified. Goffé et al. (1994) explained the presence of cookeite in these rocks, outside of its theoretical stability field, by the occurrence of saliotite, a regular 1:1 mixed layer of cookeite and paragonite. For the estimated conditions ($P > 10$–12 kbar, $T \approx 300$ °C) the association spodumene + pyrophyllite could be expected in the Li_2O-Al_2O_3-SiO_2-H_2O (LASH) system (Vidal and Goffé 1991). The phase relations in the Na_2O-Li_2O-Al_2O_3-SiO_2-H_2O (NLASH) system show that the spodumene is not stable with paragonite in the stability field of saliotite (Goffé et al. 1994). The phase relations in the NLASH system suggest that the nucleation of spodumene is probably hampered under these P-T conditions (Goffé et al. 1994). Cookeite would therefore be the stable phase.

Group F represents the highest pressures of this study: $P = 12$–16 kbar. In the phyllite-quartzite unit (Western Crete, Greece), cookeite appears in two kinds of metamorphic occurrences: metabauxites and metapelites. During this study, a second occurrence of saliotite was identified in Western Crete metabauxites, where it seems to be a relic (Goffé et al. 1994).

Chemical variability

The crystal chemistry and chemical variability of cookeite have been detailed in some previous studies (Eggleton and Bailey 1967; Cerny 1970; Bailey and Lister 1989; Jullien and Goffé 1993; Goffé et al. 1994, 1996). Chemical analyses determined in this study are reported in Table 2.

Cookeite samples analyzed in this study contain variable concentrations of Li, ranging from 3.87 wt% Li_2O (1.46 Li per formula unit, p.f.u.) in pegmatite samples from Dobra Voda to 1.68 wt% Li_2O in the Barrhorn metabauxite sample. The highest value is significantly in excess of the theoretical Li_2O content (2.85 wt%) in cookeite but is typical for pegmatitic environments. Cerny (1970) proposed a limited $AlLi_{-3}$ substitution with a maximum of about 0.2 p.f.u. Of all the samples studied, only the cookeite from Western Crete metabauxites is close to the ideal formula. Many of the samples contain cookeite with low Li_2O contents, including those from Barrhorn (1.68 wt%), Tizgarine (1.95 wt%), Western Vanoise (2.14 wt%), and Alhamilla (2.28 wt%). The Tizgarine and Barrhorn samples have either high Fe or Fe + Mg contents, and so the low Li_2O concentration can be explained by substitutions of the type $R^{2+}_2Li_{-1}Al_{-1}$, toward sudoite, and $R^{2+}SiAl_{-2}$ (Goffé et al. 1996). In the case of the Western Vanoise sample, which has a high Al_2O_3 content (47.35 wt%), $AlLi_{-3}$ substitution is probable.

Cookeite samples from Alhamilla have a detectable Na_2O content (0.15 wt%) because of fine-scale intergrowths of cookeite with paragonite and saliotite (Goffé et al. 1996). In metapelites from Western Crete, a significant Na_2O content (0.2 wt%, Crete 2, Table 2) results from numerous intergrowths of paragonite single layers observed with TEM. In the Dauphinois zone, the high Si content of cookeite (3.2 p.f.u., Table 2) was assumed to be due to systematic intergrowths with pyrophyllite (Jullien and Goffé 1993), which we confirmed in this TEM study.

TABLE 3. X-ray powder diffraction data for cookeite

hkl	I	d_{obs} (Å)	d_{calc} (Å)	hkl	I	d_{obs} (Å)	d_{calc} (Å)
Vanoise (France)				**Brittany (France)**			
002	90	14.130	14.122	002	90	14.130	14.102
004	60	7.061	7.061	004	70	7.061	7.051
006	80	4.702	4.707	006	80	4.711	4.700
102	30	4.480	4.463	020			4.474
020			4.465	$\bar{1}11$	20	4.460	4.457
$\bar{1}11$			4.460	008	70	3.527	3.526
008	70	3.531	3.530	028	20	2.763	2.769
0,0,10	10	2.824	2.824	108			2.754
$\bar{2}02$	50	2.558	2.574	200	50	2.559	2.557
200			2.560	131			2.552
131			2.549	$\bar{2}04$	50	2.500	2.500
$\bar{2}04$	60	2.506	2.505	204	90	2.317	2.318
204	100	2.320	2.319	213			2.315
213			2.317	046			2.020
142	5	2.008	2.011	2,0,$\bar{1}0$	5	2.019	2.016
0,0,14			2.006	142			2.015
$\bar{1}$,2,12			2.004	208	30	1.962	1.962
$\bar{2}28$	30	1.963	1.974	$\bar{2}40$	5	1.685	1.683
208			1.964	$\bar{3}11$			1.683
$\bar{1}$,0,14			1.958	151			1.682
$\bar{2}40$	3	1.682	1.682	$\bar{2}$,0,14			1.681
2,1,11			1.683	060	50	1.491	1.491
0,2,16	10	1.637	1.641	$\bar{2}$,2,16	5	1.455	1.455
2,0,12			1.637	2,1,15	5	1.417	1.417
$\bar{1}55$			1.633	$\bar{2}$,3,15			1.415
060	60	1.488	1.489	$\bar{2}$,0,18			1.412
162	5	1.415	1.417	$\bar{3}48$	10	1.307	1.307
$\bar{2}$,0,18			1.415	1,4,16			1.306
0,0,20			1.412	$\bar{3}$,0,16			1.304
2,0,16	10	1.371	1.378				
068			1.371				
1,4,16	3	1.300	1.306				
2,0,$\bar{2}0$			1.304				
0,4,18			1.295				

Note: Vanoise (France) unit-cell dimensions: $a = 5.150$, $b = 8.945$, $c = 28.404$ Å; $\beta = 96.79°$. Brittany (France) unit-cell dimensions: $a = 5.158$, $b = 8.926$, $c = 28.450$ Å; $\beta = 96.88°$. Space group $C2/m$. Intensities estimated visually. See text for analytical conditions.

X-RAY DATA

The crystal structure of chlorite is well known, and possible structural subunits are well documented (Brown and Bailey 1962; Eggleton and Bailey 1967; Bailey 1988). X-ray diffraction criteria for identification of dioctahedral chlorites such as cookeite are described in Bailey (1980) and Bailey and Lister (1989) and are used below. The di-trioctahedral structure of cookeite is characterized by a strong d_{060} XRD line near 1.49 Å (cf. 1.54 Å in the case of tri-trioctahedral clinochlore).

The great majority of cookeite specimens studied previously were sampled in pegmatitic environments and exhibit the most common I*a* structural unit in the terminology of Brown and Bailey (1962). The II*b* form has been described (Cerny et al. 1971) in cookeite of the Dobra Voda pegmatite, Czeck Republic, studied here. Bailey and Lister (1989) observed cookeite with the II*b* structural unit in a pegmatite from Norway, Maine, U.S.A.

During this study, we did not observe any other II*b* form. Cookeite in pegmatites from Tarn, France, and from

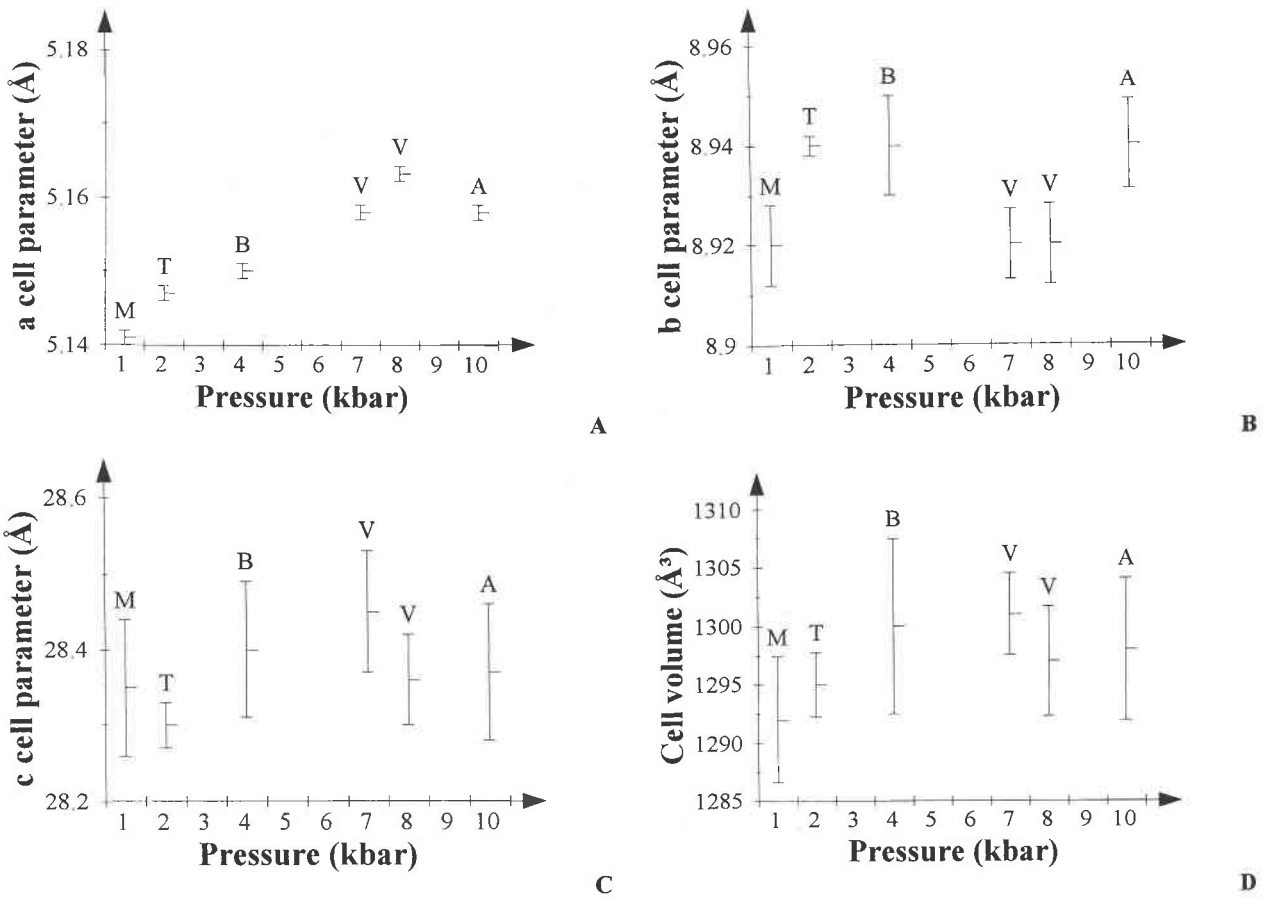

FIGURE 2. Cookeite unit-cell parameters *a*, *b*, and *c* (**A**, **B**, and **C**, respectively) and unit-cell volume (**D**) as a function of formation pressure. Sample localities are as follows: M = Maine, T = Tarn, B = Brittany, V = Vanoise, and A = Alhamilla.

Greenwood, Maine, U.S.A., has the I*a* structural unit, in good agreement with the previously determined structures in Greenwood pegmatite (Bailey and Lister 1989). The metamorphic cookeite samples all exhibit the classical I*a* structural unit, whatever the pressure domain of occurrence. For instance, the Gandolfi patterns of the two-layer Vanoise and Brittany cookeite samples (groups D and B, respectively) both show the typical I*a* form (Table 3), with a strong d_{204} diagnostic line around 2.32 Å. Accordingly, increasing pressure does not modify the type of structural units in cookeite. We confirm here that the I*a* form is the most common one for cookeite, whatever the geological context. This structure and particularly the reasons for its stability were detailed by Brown and Bailey (1962) and Bailey and Lister (1989).

The unit-cell parameters *a*, *b*, and *c* (measured at standard pressure and temperature conditions) and the unit-cell volumes of two-layer cookeite are plotted in Figure 2 as a function of formation pressure. The absence of variation with pressure suggests that the expected contraction of the single layer at high pressure is entirely relaxed at room pressure.

An increase of pressure does not cause any change in the type of structural unit, nor does it result in obvious unit-cell differences. Therefore, we explore the layer stacking sequences in cookeite in the following section.

SAED AND HRTEM RESULTS

Microstructures resulting from the cookeite layer stacking sequence are reported from specimens ranked according to increasing formation pressure. Special attention was paid to cookeite polytype periodicity, twinning, and randomly distributed stacking faults within those sequences (degree of disorder). This was accomplished by systematically orienting numerous cookeite grains of each specimen so that 00*l* and *hkl* ($k \neq 3n$) diffraction rows were simultaneously excited for each crystal.

Generally, commensurate periodicity of polytypes was determined from the reciprocal periods of equispaced diffraction spots along *hkl* ($k \neq 3n$). In contrast, the qualitative amount of randomly distributed stacking faults was estimated from continuous diffusion streaks connecting these spots along the same diffraction rows.

Only 12 regular, nonequivalent, one-layer polytypes (Brown and Bailey 1962; Spinnler et al. 1984) may exist, whereas the number of possible six-layer stacking struc-

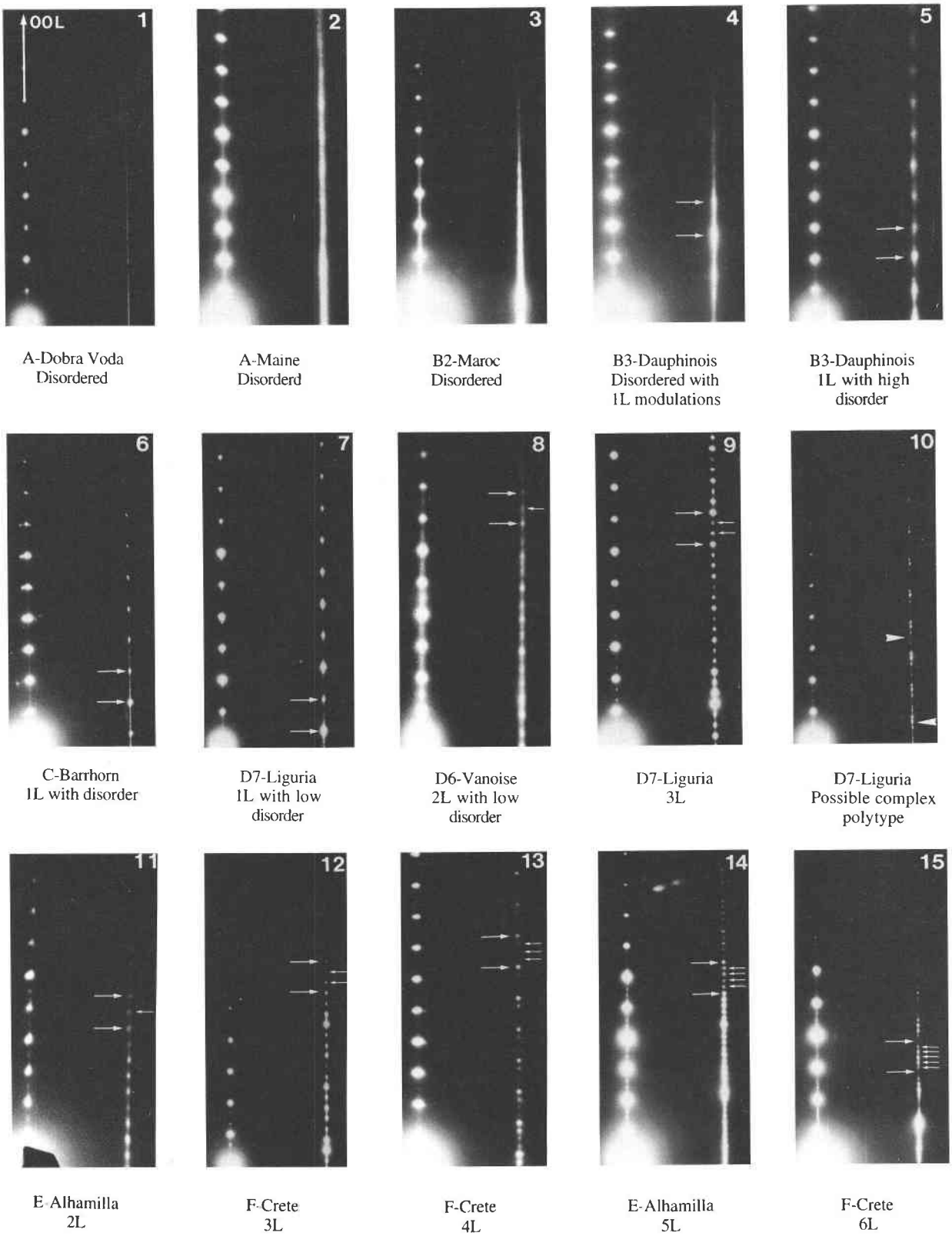

FIGURE 3. Representative SAED patterns of cookeite single crystals recorded along [100] or ⟨110⟩ zone axes. Capital letters preceding the crystal location refer to *P-T* domains as defined in Figures 1 and 8 and in Table 1.

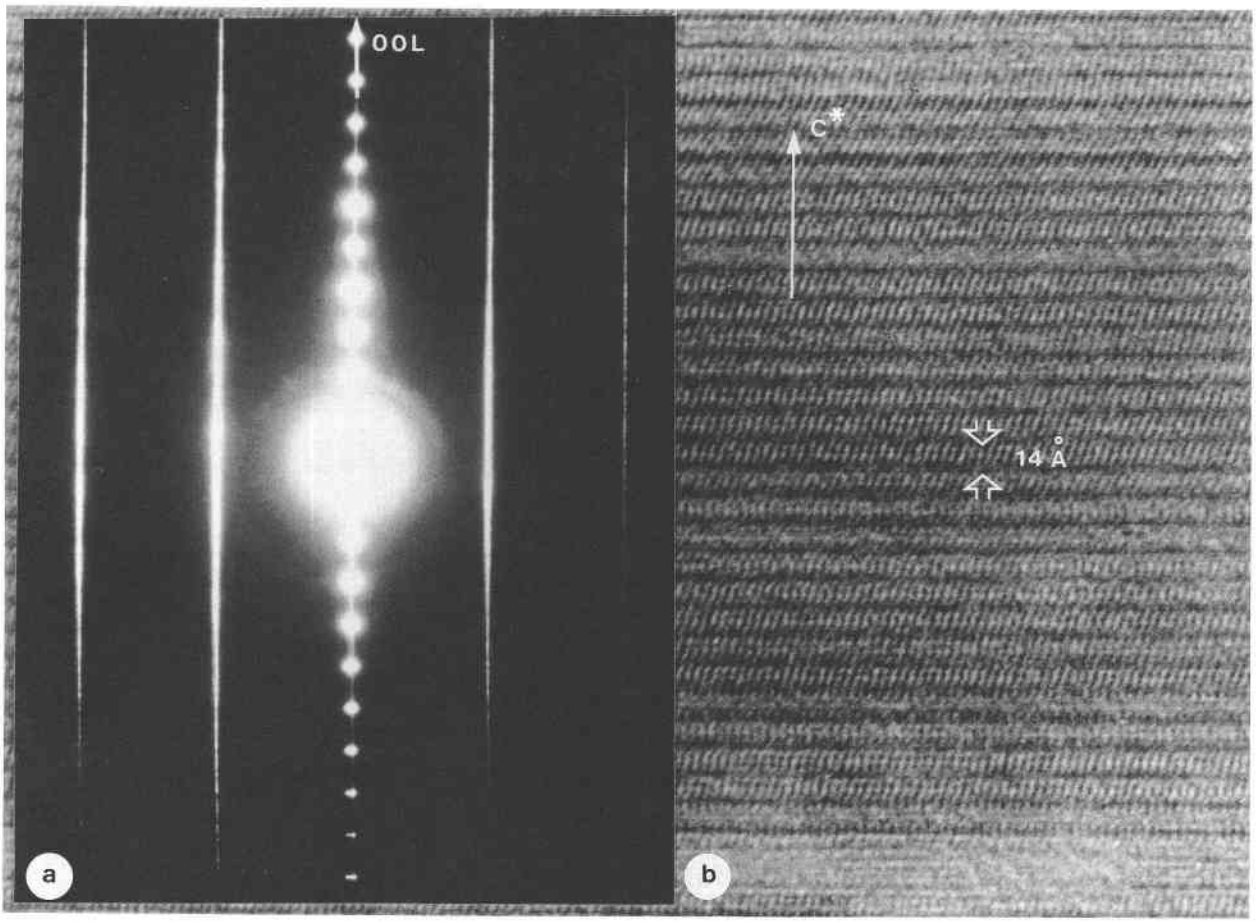

FIGURE 4. Cookeite from the Castelnau de Brassac pegmatite (Tarn, France). (**a**) SAED pattern of fully semirandom stacking as indicated by continuous hkl ($k \neq 3n$) streaks and spotty $06l$ and $33l$ row lines (not shown). (**b**) Corresponding high-resolution lattice image of a representative part of the crystal showing disordered stacking of ordered slabs, four to six single layers thick.

tures may be as large as 10^{12} (McLarnan 1981). Even if these theoretical numbers are somewhat reduced by observation of the projected stacking sequence along the viewing direction, this is certainly not sufficient to give a unique solution regarding the three-dimensional stacking sequence. Similarly, the classical Ramsdell notation could not be used because the symmetry of the polytype is not sufficiently constrained by a single structure projection (HRTEM image) or diffraction pattern (SAED). Therefore, we designate our polytypes as nL, with n as the number of layers in the repeat and L for layer.

Care was taken to insure that the SAED patterns given in Figure 3 are representative. It turns out that each single SAED represents all cases for low-pressure disordered samples, whereas integration of a set of them is necessary for high-pressure well-ordered samples, for which syntactic coalescence (intergrowth) of numerous polytypes is pronounced. All our observations are presented from low to high pressures. For comparison, the most significant SAED patterns are grouped on the diffraction table (Fig. 3), with specimens identified as in Table 1.

Pegmatitic cookeite

The cookeite samples from pegmatites display a high degree of disorder in their stacking sequences. This is marked by SAED patterns exhibiting extreme and continuous streaking along $k \neq 3n$ diffraction rows (Figs. 3.1 and 3.2). A high-resolution image of the Tarn cookeite (Fig. 4) shows 14 Å thick chlorite layers stacked without any periodicity along c^*. Occasionally the 1L polytype with numerous stacking faults appears as intensity maxima with 14 $Å^{-1}$ reciprocal periodicity along streaks in limited areas of the Maine sample. However, the great majority of cookeite samples from pegmatites are highly disordered.

Metamorphic cookeite

Cookeite from low-temperature greenschist facies rocks (group B) displays SAED patterns characteristic of highly disordered stacking sequences (Figs. 3.3–3.5), with extreme streaking along rows with $k \neq 3n$, similar to those shown previously for cookeite from pegmatites. Cookeite

from the Dauphinois area and Brittany exhibits diffraction patterns with continuous streaking in the *hkl* layer with $k \neq 3n$ and, in some cases, diffuse intensity modulations appear, with maxima at one-half or at one-third of the 1L reciprocal spacing, associated with heavy streaking. These diffraction patterns indicate significant statistical 1L, 2L, or 3L local ordering in semirandom cookeite.

In the high-temperature greenschist facies (group C), we clearly observed the appearance of ordered 1L cookeite with persistent disorder indicated on diffraction patterns by weak streaking that links 1L spots (Fig. 3.6).

Cookeite from medium-temperature blueschist facies (group D) exhibits the somewhat disordered 2L polytype in the Vanoise sample (Fig. 3.8) and 1L (Fig. 3.7), 2L twinned, or 3L (Fig. 3.9) in the Ligurian sample with rather sharp SAED patterns with or without faint streaks between Bragg reflections. Slightly disordered 1L and 2L modulations appear only in limited areas. The first indications of poorly defined long-period (complex) polytypes appear also in the Ligurian sample (Fig. 3.10), but neither the equispacing of superstructure reflections nor the commensurability of these spacings was determined.

In the Alhamilla sample, from the low-temperature blueschist facies (group E), almost all the cookeite crystals are perfectly ordered. The most common structure is the 2L polytype (Fig. 3.11). However, a rather large number of Alhamilla crystals display two reproducible five-layer

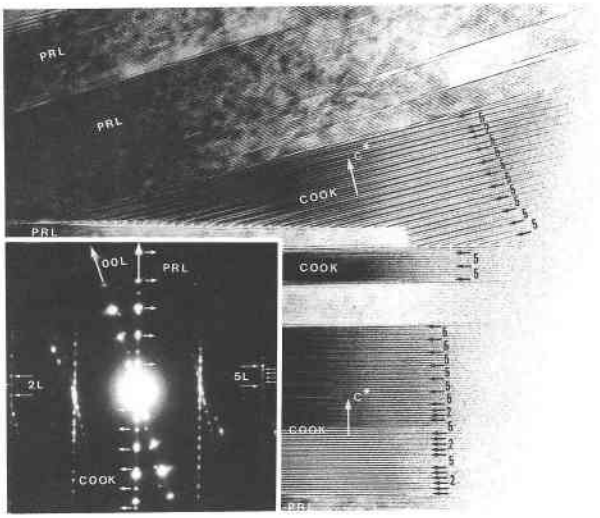

FIGURE 5. High-resolution lattice image of a typical cookeite-pyrophyllite high-pressure assemblage showing the same five-layer cookeite polytype (3 + 2 layers) in two orientations separated by a sharp grain boundary (Alhamilla, Betic Chain, Spain). The 2L polytype occurs in parallel contact with the lower 5L sequence. Insert shows SAED pattern from the region with pyrophyllite (9.3 $Å^{-1}$) and cookeite (14 $Å^{-1}$) intergrowths visible on 00*l* diffraction rows and the 5L and 2L structures of cookeite seen along the first and second lateral row lines.

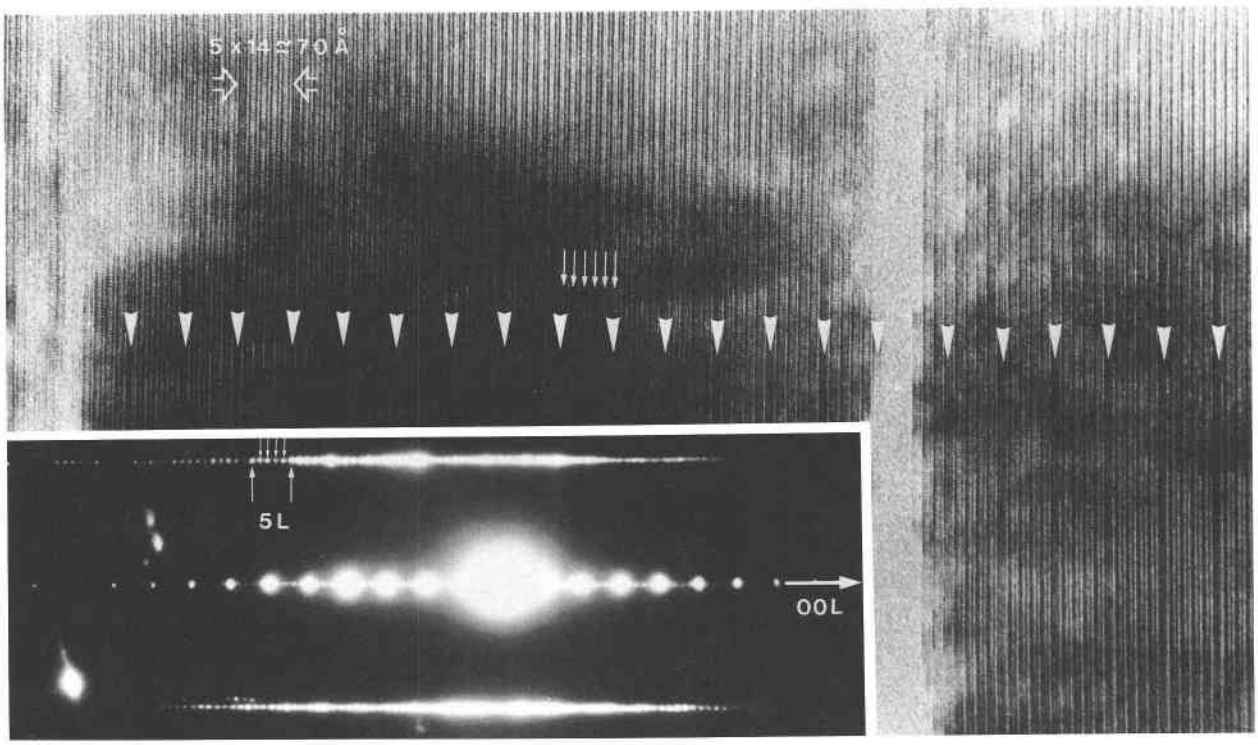

FIGURE 6. High-resolution lattice image of a second type of five-layer cookeite complex polytype (4 + 1 layer) repeating its stacking sequence more than 30 times in the original micrograph (Alhamilla, Betic Chain, Spain). Insert shows diffraction pattern.

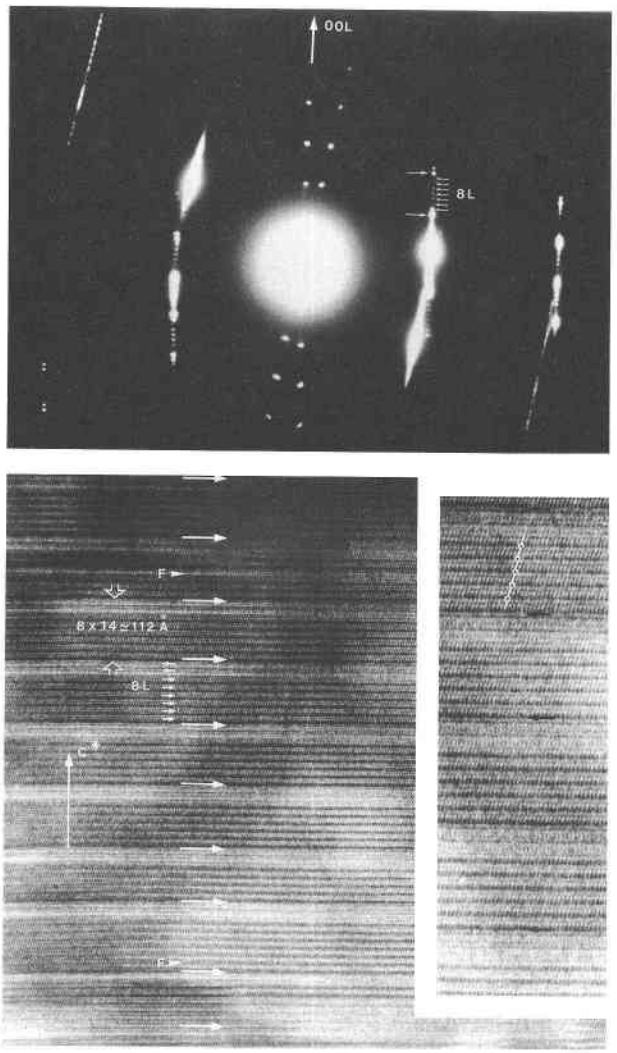

FIGURE 7. High-resolution lattice image (**bottom**) of eight-layer complex polytype (6 + 2 layers) of high-pressure cookeite [with blow-up image (lower right corner) of the eight-layer periodicity], which appears as a periodic multiple twin (Western Crete, Greece). Some stacking faults alter the sequence but keep the long periodicity in perfect registry. The SAED pattern (**top**) clearly resolves the eight-layer periodicity and also includes reflections from a second, poorly oriented, cookeite crystal, which also displays complex polytypism.

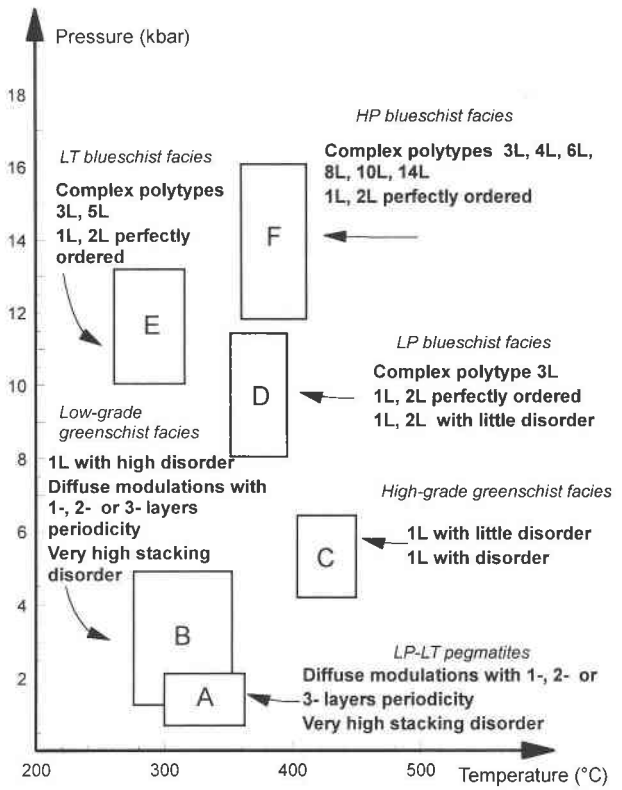

FIGURE 8. Summary of SAED and HRTEM results showing the layer-stacking ordering in cookeite, plotted as a function of *P-T* metamorphic conditions as given in Table 1.

stacking sequences as shown on SAED patterns (Fig. 3.14) and HRTEM images (Figs. 5 and 6). With $5 \times 14 \approx 70$ Å repeat distance along c^*, they may qualify as long-period polytypes. Intensity profiles recorded across the layers suggests that the first 5L stacking sequence is built up by the regular repetition of the 2L and 3L stacking sequences (Fig. 5). The other five-layer polytype (Fig. 6) displays a stacking sequence comprising four consecutive layers in seemingly parallel orientation and a fifth in a fault position with respect to the former. Therefore, this complex polytype looks like a periodically faulted 1L stacking sequence. Occasionally, some of the repeats are randomly faulted as seen in Figure 5, and regular polytype blocks on both sides of the fault are not in phase registry. This structure can be considered as integral multiples of two layers immersed in a five-layer structure. Short- and long-period polytypes of cookeite are frequently intergrown in the Alhamilla samples. Furthermore, thin slabs of disordered stacking usually represent a transitional zone between ordered regions. Pyrophyllite and cookeite are also frequently intergrown or occur as individual grains separated by low-angle rectilinear grain boundaries (Fig. 5). The (00*l*) lattice fringes are markedly rectilinear as seen also from lack of arching of 00*l* reflections. This indicates a total lack of deformation, or bending, of the layer silicates.

In the medium-temperature blueschist facies (group F), we described two samples from Western Crete (phyllite-quartzite unit) that were annealed under the same *P-T* peak conditions (370–410 °C, 12–16 kbar) but represent different geochemical environments, i.e., metapelite (Si-rich) and metabauxite (Al-rich). These cookeite samples are highly ordered without any statistically significant stacking disorder. The short-period polytypes are either the 1L, 2L, or the heavily twinned 2L polytype. Rare stacking disorder is confined to transition zones between various long-period polytypes as discussed above. We observed the 3L short-period structure (Fig. 3.12), 4L (Fig.

3.13), 6L (Fig. 3.15), 8L (Fig. 7), 10L, and probably 14L complex polytypes. These long-period polytypes are usually in syntactic coalescence (intergrowth) and all have perfectly ordered stacking sequences. As an example, the high-resolution image of the eight-layer cookeite polytype (Fig. 7) exhibits a well-ordered sequence, except for a very few stacking errors that do not cause out-of-phase positioning of the ordered sequence on either side.

Discussion

All the SAED and HRTEM results (Fig. 8) support the conclusion that pressure can play a very significant role in layer-stacking ordering. We tentatively distinguish three pressure ranges with regard to the types of polytypic structures: (1) a low-pressure range up to about 5 kbar (A and B groups, Figs. 1 and 8) in which semirandom disorder largely dominates, (2) a medium-pressure range at about $5 < P < 10$ kbar (C and lower D groups) in which the short-period polytypes 1L and 2L appear and show a decreasing amount of randomly distributed stacking faults with increasing pressure, and (3) a high-pressure range with $P > 10$ kbar (E, F, and upper D groups) in which layer-stacking order largely prevails. Mainly 2L and 3L short-period polytypes are intimately intergrown with long-period polytypes and have repeat distances that may exceed 14 layers.

We did not try HRTEM image simulations to unravel the complex three-dimensional stacking sequences because of the huge number of input trial structures giving the same projection along [100] or ⟨110⟩. Nonetheless, a superficial inspection of either (1) the intensity distribution along superstructure diffraction rows or (2) the contrast sequences in the TEM images along and across the cookeite layers, suggests that 1L, 2L, or 3L form most of the stacking sequences of complex polytypes, i.e., they structurally behave as basic structures (Baronnet and Kang 1989). The long-distance periodicity is due to the periodic occurrence of stacking faults in these basic structures. This is reminiscent of the behavior observed in trioctahedral micas (e.g. Ross et al. 1966; Takeda and Ross 1975; Bigi and Brigatti 1994) and more generally in almost all compounds exhibiting complex polytypism, e.g., SiC, ZnS, CdI_2 (Baronnet 1989; Pandey and Krishna 1982).

Although we have established a clear relationship between layer-stacking order and pressure, the structural explanation of this new phenomenon remains largely uncertain. In this respect, the following suggestions can be made. Because the cookeite host rocks commonly contain other phyllosilicates, it would be essential to check whether pyrophyllite, talc, micas, and other chlorites (sudoite, tri-trioctahedral chlorites) display the same phenomenon. Our preliminary results on pyrophyllite, talc, phengite, and sudoite, in samples studied here and in other metamorphic samples, also indicate a spectacular layer-stacking ordering as a function of pressure.

These preliminary and additional data suggest that the interlayer bonding type (ionic, hydrogen, van der Waals) does not play a critical role in layer ordering. Thus, we are left with cation-cation interaction across the interlayer space as the possible origin of ordering. The preferential shrinkage of the interlayer space under pressure (Hazen and Finger 1978; Mellini and Zanazzi 1989; Parise et al. 1994) could enhance the discriminating effect of the repulsive constraints over the stacking model of layers. Accordingly, this selective influence could favor ordered sequences that would tentatively minimize the overall cation-cation repulsive contribution to the lattice energy. However, the lack of both room-condition and high-pressure single-crystal structure determinations for cookeite prevents us from discussing the above suggestions in further detail.

Acknowledgments

The authors are greatly indebted to J.L. Banfield, A.J. Brearley, and J. Laird for their thorough and constructive reviews of the manuscript. We thank S. Nitsche for his technical assistance and advice and for use of HRTEM facilities at the CRMC². We also thank J. Cassareuil for numerous Lakeside thin sections. We are grateful to T. Theye, who kindly provided samples from Crete and Brittany, and to M.L. Bouybaouène for Tizgarine specimens. We also thank H.J. Schubnel for supplying us with cookeite samples from pegmatites of the Museum National d'Histoire Naturelle of Paris. The authors also gratefully acknowledge comments and advice on the manuscript by O. Vidal, C. Chopin, G. Ferraris, B. Devouard, and P. D'Arco.

References cited

Appleman, D.E., and Evans, H.T. (1973) Indexation and least-squares refinement of powder diffraction data. U.S. National Technical Information Service, Document PB216208.

Arsandaux, M.H. (1901) Sur quelques minéraux des environs de Brassac (Tarn, France). Bulletin de la Société française de Minéralogie, 24, 428–432.

Azañon, J.M. (1994) Metamorfismo de alta presion/baja temperatura, baja presion/alta temperatura y tectonica del complejo Alpujarride (Cordilleras betico-rifeñas), 332 p. Thesis, Universidad de Granada, Granada, Spain.

Bailey, S.W. (1980) Structure of layer silicates. In Mineralogical Society Monography, 5, 1–123.

——— (1988) Chlorites: Structures and crystal chemistry. In Mineralogical Society of America Reviews in Mineralogy, 19, 347–403.

Bailey, S.W., and Lister, J.S. (1989) Structure, composition and X-ray diffraction identification of dioctahedral chlorites. Clays and Clay Minerals, 37, 193–202.

Banfield, J.F., Bailey, S.W., and Barker, W.W. (1995) Complex polytypism: Relationships between serpentine structural characteristics and deformation. American Mineralogist, 80, 1116–1131.

Baronnet, A. (1989) Polytypism and crystal growth of inorganic crystals. In NATO ASI Series, B, vol. 210, 197–204.

——— (1992) Polytypism and stacking disorder. In Mineralogical Society of America Reviews in Mineralogy, 27, 231–288.

Baronnet, A., and Kang, Z.C. (1989) About the origins of mica polytypes. Phase Transitions, 16/17, 477–493.

Bigi, S., and Brigatti, M.F. (1994) Crystal chemistry and microstructures of plutonic biotite. American Mineralogist, 79, 63–72.

Bons, A.-J., and Schryvers, D. (1989) High-resolution electron microscopy of stacking irregularities in chlorites from the central Pyrenees. American Mineralogist, 74, 1113–1123.

Bouybaouène, M.L. (1993) Etude pétrologique des métapélites des Sebtides supérieures, Rif'interne, Maroc: Une évolution métamorphique de haute pression, 150 p. Thèse, Université Mohammed V, Rabat, Morocco.

Brammal, A., Leech, J.G.C., and Bannister, F.A. (1937) The paragenesis

of cookeite and hydromuscovite associated with gold at Ogofan, Carmarthenshire. Mineralogical Magazine, 24, 507.

Brown, B.E., and Bailey, S.W. (1962) Chlorite polytypism: I. Regular and semi-random one-layer structures. American Mineralogist, 47, 819–850.

——— (1963) Chlorite polytypism: II. Crystal structure of a one-layer Cr-chlorite. American Mineralogist, 48, 42–61.

Cerny, P. (1970) Compositional variation in cookeite. Canadian Mineralogist, 10(4), 636–647.

Cerny, P., Povondra, P., and Stanek, J. (1971) Two cookeites from Czechoslovakia: A boron-rich variety and a II*b* polytype. Lithos, 4, 7–15.

Cliff, G., and Lorimer, G.W. (1975) The quantitative analysis of thin specimens. Journal of Microscopy, 103, 203–207.

Eggleton, R.A., and Bailey, S.W. (1967) Structural aspects of dioctahedral chlorite. American Mineralogist, 52, 673–689.

Ferrow, E.A., London, D., Goodman, K.S., and Veblen, D.R. (1990) Sheet silicates of the Lawler Peak granite, Arizona: Chemistry, structural variation and exsolution. Contributions to Mineralogy and Petrology, 105, 491–501.

Gillet, P., and Goffé, B. (1988) On the significance of aragonite in Western Alps. Contributions to Mineralogy and Petrology, 99, 70–81.

Goffé, B. (1977) Présence de cookéite dans les bauxites métamorphiques du Dogger de la Vanoise (Savoie). Bulletin de la Société française de Minéralogie et de Cristallographie, 100, 254–257.

——— (1979) La lawsonite et les associations à pyrophyllite-calcite dans les sédiments alumineux du Briançonnais: Premières occurrences. Comptes Rendus de l' Académie des Sciences de Paris, 289, Série D, 813–816.

——— (1980) Magnésiocarpholite, cookéïte et euclase dans les niveaux continentaux métamorphiques de la zone Briançonnaise: Données métamorphiques et nouvelles occurences. Bulletin de la Société française de Minéralogie et de Cristallographie, 103, 297–302.

——— (1982) Définition du faciès Fe-Mg carpholite-chloritoïde, un marqueur du métamorphisme de HP-BT dans les métasédiments alumineux, 212 p. Thèse d'Etat, Université de Paris VI, France.

——— (1984) Le faciès à carpholite-chloritoïde dans la couverture briançonnaise des Alpes ligures: Un témoin de l'évolution tectono-métamorphique régionale. Memoria Società Geologica Italiana, 28, 461–479.

Goffé, B., Murphy, W.M., and Lagache, M. (1987) Experimental transport of Si, Al and Mg in hydrothermal solutions: An application to vein mineralization during high-temperature–low-pressure metamorphism in French Alps. Contributions to Mineralogy and Petrology, 97, 438–450.

Goffé, B., Baronnet, A., and Morin, G. (1994) La saliotite, interstratifié régulier 1:1 cookéite/paragonite: Un nouveau phyllosilicate du métamorphisme de haute pression et basse température. European Journal of Mineralogy, 6, 897–911.

Goffé, B., Azañon, J.M., Bouybaouene, M.L., and Jullien, M. (1996) Metamorphic cookeites in Alpine metapelites from the Rif (Morocco) and Betic chain (Spain). European Journal of Mineralogy, in press.

Hazen, R.M., and Finger, L.W. (1978) The crystal structures and compressibilities of layer minerals at high pressure: II. Phlogopite and chlorite. American Mineralogist, 63, 293–296.

Jolivet, L., Goffé, B., Monié, P., Patriat, M., Truffert, C., and Bonneau, M. (1996) Miocene detachment in Crete and exhumation of high pressure metamorphics. Tectonics, in press.

Jullien, M., and Goffé, B. (1993) Occurrences de cookéite et de pyrophyllite dans les schistes du Dauphinois (Isere, France): Conséquences sur la repartition du métamorphisme dans les zones externes Alpines. Schweizerische Mineralogische und Petrographische Mitteilungen, 73, 357–363.

Lacroix, A. (1915) Manandonite et Cookéite. Bulletin de la Société française de Minéralogie, 38, 142–146.

Lister, J.S., and Bailey, S.W. (1967) Chlorite polytypism: IV. Regular two-layer structures. American Mineralogist, 52, 1614–1631.

Maresch, W.V., Massonne, H.J., and Czank, M. (1985) Ordered and disordered chlorite/biotite interstratifications as alteration product of chlorite. Neues Jahrbuch für Mineralogie Abhandlungen, 152, 79–100.

McLarnan, T.J. (1981) The number of polytypes in close-packings and related structures. Zeitschrift für Kristallographie, 155, 269–291.

Mellini, M., and Menichini, R. (1985) Proportionality factors of thin film TEM/EDS microanalyses of silicate minerals. Rendiconti della Società Italiana di Mineralogia e Petrologia, 40, 261–266.

Mellini, M., and Zanazzi, P.R. (1989) Effects of pressure on the structure of lizardite-1*T*. European Journal of Mineralogy, 1, 13–19.

Messiga, B., Oxilia, M., Piccardo, G.B., and Vanossi, M. (1982) Fasi metamorfiche e deformazioni alpine nel Brianzonese e nel Pre-Piemontese–Piemontese esterno delli Alpi liguri: Un possibile modello evolutivo. Rendiconti della Società Italiana di Mineralogia e Petrologia, 38(1), 261–280.

Pandey, D., and Krishna, P. (1982) Polytypism in close-packed structures. Current Topics in Materials Science, 9, 415–491.

Paradis, S., Velde, B., and Nicot, E. (1983) Chloritoid-pyrophyllite-rectorite facies rocks from Brittany, France. Contributions to Mineralogy and Petrology, 83, 342–347.

Parise, J.B., Leinenweber, K., Weidner, D.J., Tan, K., and Von Dreele, R.B. (1994) Pressure-induced H bonding: Neutron diffraction study of brucite, $Mg(OD)_2$, to 9.3 GPa. American Mineralogist, 79, 193–196.

Penfield, S.L. (1894) On cookeite from Paris and Hebron, Maine. Bulletin de la Société française de Minéralogie, 17, 223–224.

Ross, M., Takeda, H., and Wones, D.R. (1966) Mica polytypes: Systematic description and identification. Science, 151, 191–193.

Saliot, P., and Velde, B. (1982) Phengite composition and post-nappe high-pressure metamorphism in the Pennine zone of the French Alps. Earth and Planetary Sciences Letters, 57, 133–138.

Sartori, M. (1988) L'unité du Barrhorn (zone pennique, Valais, Suisse), 150 p. Thèse de Doctorat, Université de Lausanne, Lausanne, Switzerland.

Schreyer, W., Medenbach, O., Abraham, K., Gebert, W., and Müller, W.F. (1982) Kulkeite, a new metamorphic phyllosilicate mineral: Ordered 1:1 chlorite/talc mixed-layer. Contributions to Mineralogy and Petrology, 80, 103–109.

Shirozu, H., and Bailey, S.W. (1965) Chlorite polytypism: III. Crystal structure of an orthohexagonal iron chlorite. American Mineralogist, 50, 868–885.

Spinnler, G.E., Self, P.G., Iijima, S., and Buseck, P.R. (1984) Stacking disorder in clinochlore chlorite. American Mineralogist, 69, 252–263.

Takeda, H., and Ross, M. (1975) Mica polytypism: Dissimilarities in the crystal structures of coexisting 1*M* and $2M_1$ biotite. American Mineralogist, 60, 1030–1040.

Theye, T. (1988) Aufsteigende Hochdruckmetamorphose in Sedimenten der Phyllit-Quartzit-Einheit Kretas und Peloponnes, 224 p. Dissertation, Technische Universität Carolo Wilhelmina zu Braunschweig, Brunswick, Germany.

Theye, T., Seidel, E., and Vidal, O. (1992) Carpholite, sudoite, and chloritoid in low-temperature high-pressure metapelites from Crete and the Peloponnese, Greece. European Journal of Mineralogy, 4, 487–507.

Veblen, D.R. (1983) Microstructures and mixed layering in intergrown wonesite, chlorite, talc, biotite, and kaolinite. American Mineralogist, 68, 566–580.

Veblen, D.R., and Ferry, J.M. (1983) A TEM study of the biotite-chlorite reaction and comparison with petrologic observations. American Mineralogist, 68, 1160–1168.

Vidal, O., and Goffé, B. (1991) Cookeite experimental study and thermodynamical analysis of its compatibility relations in the Li_2O-Al_2O_3-SiO_2-H_2O system. Contributions to Mineralogy and Petrology, 108, 72–81.

Vidal, O., Goffé, B., and Theye, T. (1992) Experimental study of the stability of sudoite and magnesiocarpholite and calculation of a new petrogenetic grid for the system FeO-MgO-Al_2O_3-SiO_2-H_2O. Journal of Metamorphic Geology, 10, 603–614.

Vrublevskaja, Z.V., Delitsin, I.S., Zvyagin, B.B., and Soboleva, S.V. (1975) Cookeite with a perfect regular structure, formed by bauxite alteration. American Mineralogist, 60, 1041–1046.

Manuscript received December 1, 1994
Manuscript accepted September 1, 1995